SUPPLEMENTARY RESULTS

Exocyst requirements for the constitutive and regulated insertion of functional AMPARs at synapses (rectification analysis)

As a functional test for the role of the exocyst in the constitutive and regulated synaptic delivery of AMPARs, we carried out electrophysiological experiments in which the presence of recombinant receptors at synapses is detected from their inward rectification properties (electrophysiological tagging). Briefly, the constitutive delivery of AMPARs is monitored by expressing a recombinant GluR2 subunit with a point mutation at the channel pore (R607Q), which abolishes outward currents at positive membrane potentials. In this assay, an increase in the rectification index of synaptic transmission (defined here as the ratio between AMPAR responses at -60 mV versus +40 mV), indicates that homomeric recombinant AMPARs have been delivered into synapses (these recordings were carried out separately for transfected and untransfected cells, since the rectification index reflects an intrinsic property of the AMPARs present at synapses). As shown in Supplementary Fig. 6A, expression of GluR2(R607Q)-GFP produced inward rectification of synaptic transmission, as expected. This rectification was completely blocked by co-expression of the recombinant receptor with Exo70-N (Supplementary Fig. 6A), indicating that Exo70 function is absolutely required for the constitutive delivery of AMPARs into synapses. Importantly, co-expression of GluR2(R607Q) and full-length Exo70 did not block the increase in rectification, demonstrating that the effect observed with Exo70-N is not due to inefficient co-expression of two recombinant proteins.

The regulated delivery of AMPARs can be monitored by co-expressing recombinant GluR1 with a constitutively active form of αCaMKII (tCaMKII), which drives receptor insertion at synapses. As shown in Supplementary Fig. 6B, the increase in rectification observed with

tCaMKII plus GluR1-GFP was completely blocked by co-expression with Exo70-N or Sec8-Ct, indicating that Exo70 and Sec8 are also necessary for the CaMKII-dependent delivery of AMPARs into synapses. Again, as control for co-transfection efficiency, expression of GluR1-GFP, tCaMKII and full-length Exo70 did not block rectification.

These electrophysiological results reinforce our fluorescence imaging data, and confirm that the exocyst is required for the functional insertion of all AMPAR populations at synapses.

SUPPLEMENTARY METHODS

DNA constructs and expression of recombinant proteins

Mouse full-length Exo70 and Exo70-N (amino acids 1 to 384) were prepared as fusion proteins upstream from EGFP using pEGFP-N1 (Clontech). Mouse full-length Sec8 and Sec8 C-terminus (last 16 amino acids) were fused downstream from EGFP using pEGFP-C1 (Clontech). The truncated version of the Sec8 C-terminus (Sec8-Ct-Δ4) lacks the last four amino acids (-ITTV). The GFP-tagged AMPA receptor subunits (GluR1-GFP and GluR2-R607Q-GFP) and the truncated αCaMKII construct were prepared as previously described (Shi et al., 2001). RFP fusion constructs are equivalent to their GFP counterparts, but using the red fluorescence protein variant tdimer2(12) (Campbell et al., 2002), generously provided by R. Tsien (UCSD, CA). NR2B-Ct-RFP was generated by fusing the last 16 amino acids of NR2B downstream from RFP.

Organotypic slice cultures are prepared from young rats (postnatal day 5 to 6) and placed on semiporous membranes for 4 to 7 days (Gahwiler et al., 1997). Expression of single recombinant proteins was carried out with the Sindbis virus expression system (Gerges et al., 2005; Schlesinger, 1993). For co-expression of two or more proteins we used the biolistic delivery method (Lo et al., 1994) using plasmids bearing the cytomegalovirus (CMV) promoter

(Gerges et al., 2005). We have observed 100% co-expression efficiency with this system, as judged from co-transfection experiments with fluorescent proteins of different colors, such as green and red fluorescence proteins. Recombinant proteins were expressed for 36 hours when using AMPA receptor subunits, or for 15 hours in the rest of the cases. Neurons remain morphologically and electrophysiologically intact during these expression times. All animal care protocols were approved by the University of Michigan.

Electrophysiology

The recording chamber was perfused with 119 mM NaCl, 2.5 mM KCl, 4 mM $CaCl_2$, 4 mM $MgCl_2$, 26 mM $NaHCO_3$, 1 mM NaH_2PO_4, 11 mM glucose, 0.1 mM picrotoxin and 2 μM 2-chloroadenosine, at pH 7.4, and gassed with 5% CO_2, 95% O_2. Patch recording pipettes (3-6 MΩ) were filled with 115 mM cesium methanesulfonate, 20 mM CsCl, 10 mM HEPES, 2.5 mM $MgCl_2$, 4 mM Na_2ATP, 0.4 mM Na_3GTP, 10 mM sodium phosphocreatine and 0.6 mM EGTA, at pH 7.25. For peptide infusion experiments (Fig. 2) 1 mM of the indicated peptide, 100 μM leupeptin, 10 μM pepstatin, 10 μM antipain and 10 μM chemostatin were included in the intracellular solution. For rectification experiments (Supplementary Fig. 6), 0.1 mM spermine was added in the intracellular solution, and 0.1 mM DL-2-amino-5-phosphonovaleric acid was present in the bath solution.

Confocal microscopy

Confocal images of neurons transfected with different fluorescent proteins were taken with an Olympus FV 500 confocal microscope. FluoView software was used for image acquisition, and ImageJ for three-dimensional reconstruction and fluorescence intensity

quantifications. Surface immunostaining of GluR1- and GluR2-GFP was carried in non-permeabilized conditions using anti-GFP (Roche) and biotinylated anti-mouse (Sigma) antibodies, and streptavidin coupled to Cy5 (Amersham Biosciences). Receptor distribution at spines and adjacent dendrites was quantified with line plots of fluorescence intensity across spine heads and the adjacent dendritic shaft. The fluorescence intensity peak at each compartment was calculated after background subtraction. Surface ratios were calculated as the ratio between the Cy5 signal (surface receptor) and GFP signal (total receptor) (Brown et al., 2005; Gerges et al., 2004; Gerges et al., 2005).

Electron microscopy

Hippocampal slices were fixed and processed for osmium-free post-embedding immunogold labeling essentially as described previously (Phend et al., 1995). AMPARs were labeled with anti-GluR2/3 antibody (Chemicon) and an anti-rabbit antibody coupled to 10-nm gold particles (Electron Microscopy Sciences). Electron micrographs were obtained with a Philips CM-100 transmission electron microscope and a Kodak 1.6 Megaplus digital camera.

Immunoprecipitation experiments from synaptosomal preparations

Hippocampal extracts were prepared in homogenization buffer containing 320 mM sucrose, 2 mM DTT, 2 mM EDTA, 4 mM HEPES, pH 7.4, 0.1 mM PMSF, 1 μg/ml aprotinin, 1 μg/ml leupeptin, 1 μg/ml antipain and 1 μg/ml pepstatin. The homogenates are spun down at 1,100 g for 10 min. The resultant supernatant was further spun down at 9,200 g. The pellet (synaptosomal fraction) is then solubilized in the same buffer in the presence of 1% Triton X-100 for immunoprecipitation. Antibodies used for western blot analysis and immunoprecipitation

experiments were anti-sec6 (Stressgen), anti-sec8 (BD Biosciences), anti-Exo70 (generous gift from S. C. Hsu, Rutgers University, NJ), anti-GluR1 (Chemicon), anti-GluR2/3 (Chemicon), anti-NR1 (Chemicon), anti-NR2A/B (Chemicon), anti-mGluR2/3 (Upstate Biotechnology), anti-Rab8 (BD Biosciences), anti-Rab11 (Zymed), A.V. peptide (rabbit anti-GFP; BD Biosciences), anti-GFP (Roche), anti-Myosin Va (Sigma), anti-PSD95 (Upstate Biotechnology), anti-αCaMKII (Upstate Biotechnology) and anti-Rho (BD Biosciences).

PSD fractionations

Hippocampal extracts were prepared in homogenization buffer containing 5 mM HEPES, pH 7.4, 1 mM $MgCl_2$, 0.5 mM $CaCl_2$, 1 mM NaF, 0.1 mM PMSF, 1 μg/ml aprotinin, 1 μg/ml leupeptin, 1 μg/ml antipain and 1 μg/ml pepstatin (buffer A). Synaptosomal and PSD fractionations were carried out essentially as previously described (Peng et al., 2004). Briefly, 30-45 hippocampal slices were homogenized in Buffer A using a Teflon homogenizer. The homogenates are spun down at 1,400 g for 10 min to produce a supernatant (S1) and a pellet (P1). The pellet (P1) is resuspended in buffer A and spun down at 700 g to produce the cellular debris pellet (P1') and a supernatant (S1'). S1 and S1' were combined and spun down at 13,800 g. The pellet of this centrifugation constitutes the synaptosomal fraction (P2). To isolate the PSD fraction, P2 was resuspended in buffer B, which contains 0.32 M sucrose, 6 mM Tris-HCl, pH 8.0, 1 mM NaF, 0.1 mM PMSF, 1 μg/ml aprotinin, 1 μg/ml leupeptin, 1 μg/ml antipain and 1 μg/ml pepstatin, and then loaded unto a discontinuous sucrose gradient (0.85 M, 1 M and 1.15 M sucrose in buffer B). The interface of the 1 M/1.15 M sucrose layers was collected after ultracentrifugation at 82,500 g for 2 hours. This interface was mixed with an equal amount of

buffer C (6 mM Tris-HCl, pH 8.1, and 1% Triton X-100) for 30 min. The Triton-insoluble fraction (PSD) was collected by ultracentrifugation at 32,800 g for 30 minutes.

Peptide synthesis and purification

Peptides were manually prepared and analyzed in a manner consitent with standard Fmoc-based solid-phase peptide synthesis protocols (Chan and White, 2000). N-αFluorenylmethoxycarbonyl amino acids and Val Novasyn TGA resin were purchased from NovaBiochem. DIPCDI and DIPEA were from Acros; HOBt and HBTU were from NovaBiochem; dimethylformamide was from Acros. Dichloromethane, propan-2-ol, acetic acid and diethyl ether were obtained from Fisher. Piperidine was obtained from Alfa Aesar. After synthesis, collected peptides were dissolved in water and lyophilized. A small amount of the crude peptide (1 mg) was submitted for mass spectral analysis (ESI-MS and MALDI-TOF mass analysis) (see Supplementary Fig. 3A). The peptide was purified by RP-HPLC (Phenomenex column, 4.6 x 250 mm, pore size 1 Å). The solvent system used was 60:40 water (0.1% TFA):methanol. The peptide-containing fractions were identified and combined, followed by lyophilization. A small scale, analytical HPLC was performed subsequently to confirm the purity and homogeneity of the isolated peptides (see Supplementary Fig. 3B). Peptide sequences were as follows. Sec8 C-t: KDKKITTV; NR2B C-t: LSSIESDV; Sec8-mut C-t: KDKKIATA.

Statistical analyses

Comparison of electrophysiological responses between pairs of infected and uninfected neurons (Fig. 1) and fluorescence intensity in dendrite-spine pairs (Figs. 5 and 6) was carried out using the paired non-parametric Wilcoxon test. Mean values of GFP fluorescence in distal

dendrites (Fig. 4), rectification index of AMPA receptor synaptic responses (Supplementary Fig. 6), protein accumulation at PSD fractions (Fig. 7) and PSD immunogold labeling (Fig. 8B) were compared using two-side unpaired t-tests. Comparison of cumulative distributions (Figs. 5 and 8C) was carried out with the Kolmogorov-Smirnov test. Error bars represent standard error of the mean in all figures.

REFERENCES

Brown, T.C., Tran, I.C., Backos, D.S. and Esteban, J.A. (2005) NMDA receptor-dependent activation of the small GTPase Rab5 drives the removal of synaptic AMPA receptors during hippocampal LTD. *Neuron*, **45**, 81-94.

Campbell, R.E., Tour, O., Palmer, A.E., Steinbach, P.A., Baird, G.S., Zacharias, D.A. and Tsien, R.Y. (2002) A monomeric red fluorescent protein. *Proc Natl Acad Sci U S A*, **99**, 7877-7882.

Chan, W.C. and White, P.D. (2000) *Fmoc Solid Phase Peptide Synthesis: A Practical Approach*. Oxford University Press.

Gahwiler, B.H., Capogna, M., Debanne, D., McKinney, R.A. and Thompson, S.M. (1997) Organotypic slice cultures: a technique has come of age. *Trends Neurosci*, **20**, 471-477.

Gerges, N.Z., Backos, D.S. and Esteban, J.A. (2004) Local control of AMPA receptor trafficking at the postsynaptic terminal by a small GTPase of the Rab family. *J Biol Chem*, **279**, 43870-43878.

Gerges, N.Z., Brown, T.C., Correia, S.S. and Esteban, J.A. (2005) Analysis of Rab protein function in neurotransmitter receptor trafficking at hippocampal synapses. *Methods Enzymol*, **403**, 153-166.

Lo, D.C., McAllister, A.K. and Katz, L.C. (1994) Neuronal transfection in brain slices using particle-mediated gene transfer. *Neuron*, **13**, 1263-1268.

Peng, J., Kim, M.J., Cheng, D., Duong, D.M., Gygi, S.P. and Sheng, M. (2004) Semi-quantitative proteomic analysis of rat forebrain postsynaptic density fractions by mass spectrometry. *J Biol Chem*.

Phend, K.D., Rustioni, A. and Weinberg, R.J. (1995) An osmium-free method of epon embedment that preserves both ultrastructure and antigenicity for post-embedding immunocytochemistry. *J Histochem Cytochem*, **43**, 283-292.

Schlesinger, S. (1993) Alphaviruses--vectors for the expression of heterologous genes. *Trends Biotechnol*, **11**, 18-22.

Shi, S., Hayashi, Y., Esteban, J.A. and Malinow, R. (2001) Subunit-specific rules governing AMPA receptor trafficking to synapses in hippocampal pyramidal neurons. *Cell*, **105**, 331-343.

SUPPLEMENTARY FIGURE LEGENDS

Supplementary Figure 1. Truncated Exo70 (Exo70-N) interacts with endogenous exocyst subunit Sec8. Immunoprecipitations were carried out from Triton-solubilized synaptosomal preparations of CA1 hippocampal slices (similar to Fig. 3) expressing Exo70-N (+) or control, uninfected slices (-). Antibodies for immunoprecipiation were anti-sec8 or non-immune (N.I.), as indicated. Total soluble protein in the synaptosomes (10% input) and immunoprecipitated fractions were analyzed by immunoblotting using anti-sec8 (top panel), anti-sec6 (middle panel) and anti-GFP (bottom panel). The recombinant protein, Exo70-N-GFP, is detected with the anti-GFP antibody. The heavy chain of the immunoprecipitation antibody (IgG) and a non-specific band associated to the non-immune antibody (asterisk) are also indicated in the bottom panel.

Supplementary Figure 2. Effect of exocyst subunit expression on cell input resistance and holding current. Average input resistance (**A**) and holding current (**B**) from uninfected cells and their corresponding infected pairs expressing Sec8-Ct, Sec8-wt, Sec8-Ct-Δ4, Exo70-N and Exo70-wt, as indicated (same constructs used in Fig. 1). Error bars represent standard error of the mean. n stands for the number of cells. None of the differences was statistically significant, according to the *t* test.

Supplementary Figure 3. Analysis of identity and purity of peptides Sec8 C-t, NR2B C-t and Sec8-mut C-t. (**A**). Mass spectral analysis (ESI-MS and MALDI-TOF) of the indicated peptides. Calculated and found m/z values for the peptides are indicated. (**B**) RP-HPLC elution profiles of Sec8 C-t, NR2B C-t and Sec8-mut C-t in 60:40 water (0.1% TFA):methanol.

Supplementary Figure 4. Analysis of GluR2-GFP dendritic transport. A. Schematic representation of the quantification procedure. GFP fluorescence intensity is measured along the main apical dendrite as a function of the distance from the cell soma. Fluorescence values at any given distance (x) are normalized to the value at the cell soma (0 μm, 100% fluorescence) after background subtraction. **B** Line plot representation of the quantification of GluR2-GFP dendritic transport as described in A. Data are presented as mean (thick lines) ± s.e.m. (thin dashed lines) for the expression of GluR2-GFP alone (black lines), GluR2-GFP plus Exo70-N-RFP (red lines), GluR2-GFP plus Sec8-Ct-RFP (blue lines) or GluR2-GFP plus NR2B-Ct-RFP (green lines). n represents number of cells.

Supplementary Figure 5. Effect of Sec8-Ct and NR2B-Ct on local receptor trafficking at dendritic spines. Scatter plots of GluR2-GFP surface and total distribution at spines and adjacent dendritic shafts in the presence of Sec8-Ct (top panels) or NR2B-Ct (bottom panels), from the data set shown in Fig. 6A-C of the main text (GluR2 + Sec8-Ct and GluR2 + NR2B-Ct). Each point in these plots represents one pair of spine and adjacent dendrite. Points below the diagonal line represent pairs in which fluorescence intensity was lower in the spine than in the dendrite. Fluorescence intensity signals for surface receptor (Cy5 channel), total receptor (GFP channel) and surface ratio (Cy5/GFP) were calculated as described in the main text. All fluorescence values are normalized to the mean fluorescence intensity at dendrites. In the case of Sec8-Ct, all three parameters (surface –A–, total –B– and surface ratio –C–) yield significantly less fluorescence intensity at spines than at dendrites, according to the Wilcoxon test. In the case of NR2B-Ct, the reduction of spine surface (D) and surface ratio (F) were statistically significant,

but of much less magnitude than the effects observed with Sec8-Ct. NR2B-Ct did not significantly alter total AMPA receptor presence at spines (E).

Supplementary Figure 6. Rectification analysis for the role of the exocyst in the constitutive and regulated insertion of functional AMPARs at synapses. **A, B.** Rectification indexes were calculated as the ratio between the amplitude of AMPAR synaptic responses at -60 mV over the amplitude at +40 mV. Endogenous receptors conduct current at -60 mV and +40 mV, whereas recombinant (homomeric) receptors conduct only at negative membrane potentials (inward rectification). Therefore, delivery of the recombinant receptors is accompanied by an increase in the rectification index. (**A**) Average rectification values obtained from control untransfected neurons or from neurons transfected with GluR2(R607Q), GluR2(R607Q) plus Exo70-N or GluR2(R607Q) plus Exo70-wt. (**B**) Average rectification values obtained from neurons transfected with GluR1 plus a constitutively active αCaMKII (tCaMKII), or in combination with Exo70-N, Exo70-wt or Sec8-Ct, as indicated. Inset, sample traces of evoked AMPA receptor mediated synaptic responses recorded at –60 mV and +40 mV from control or transfected cells as indicated. Scale bars, 20 pA and 20 ms.

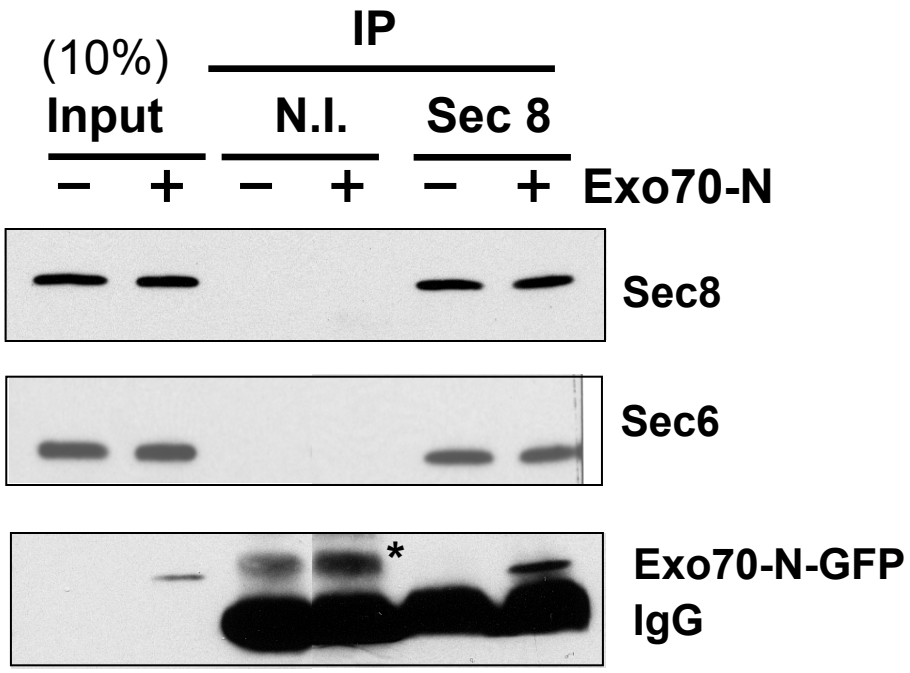

Supplementary Figure 1 (Esteban)

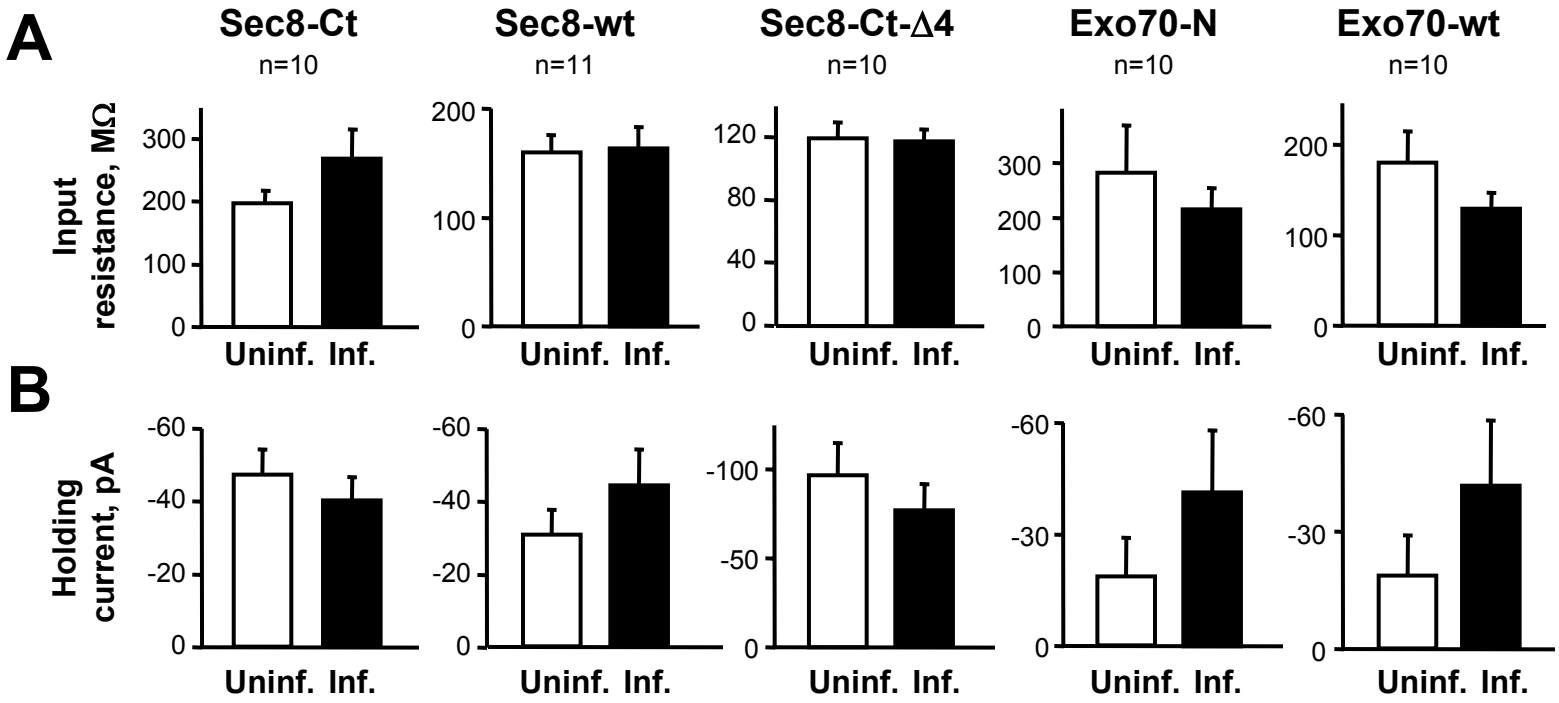

Supplementary Figure 2 (Esteban)

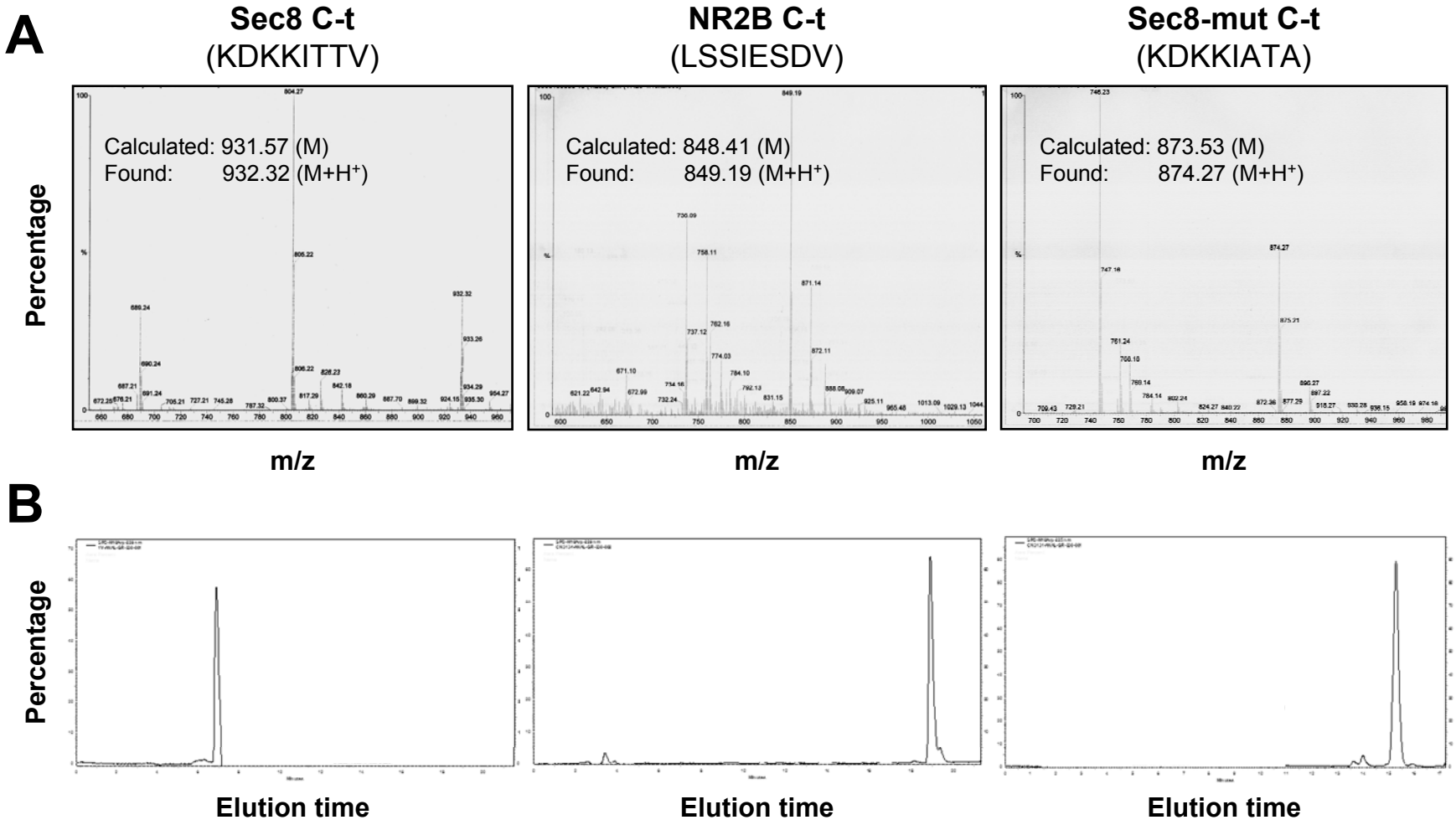

Supplementary Figure 3 (Esteban)

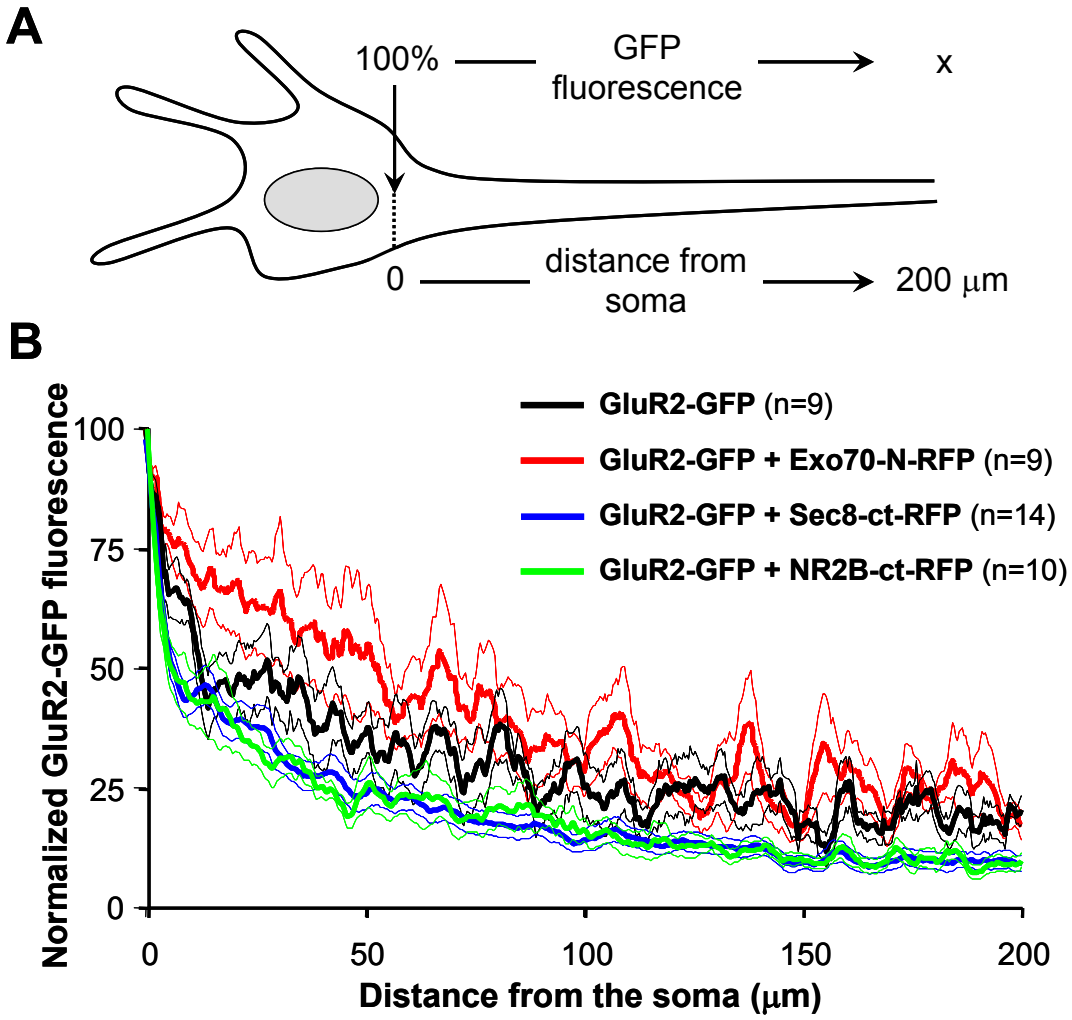

Supplementary Figure 4

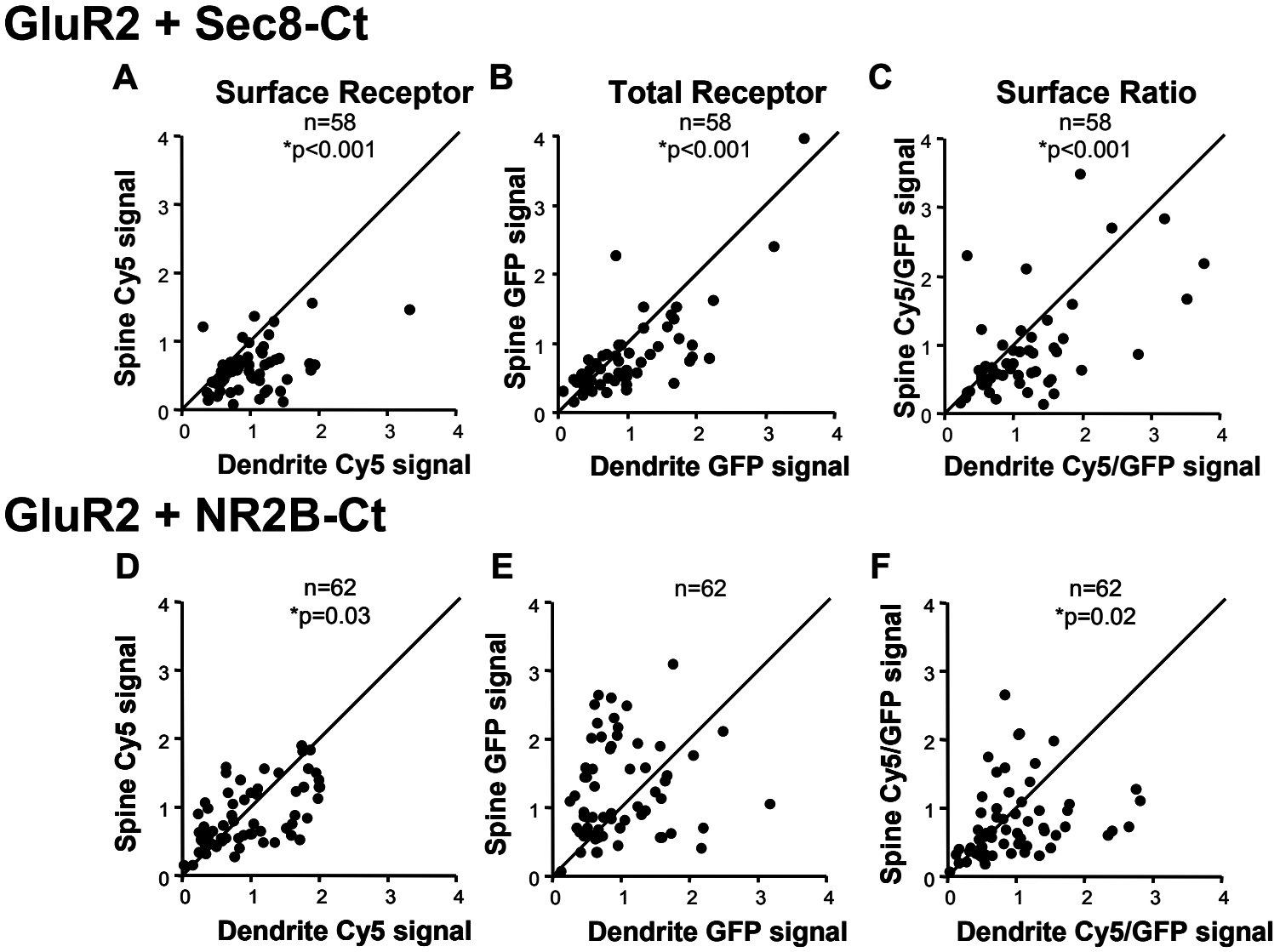

Supplementary Figure 5 (Esteban)

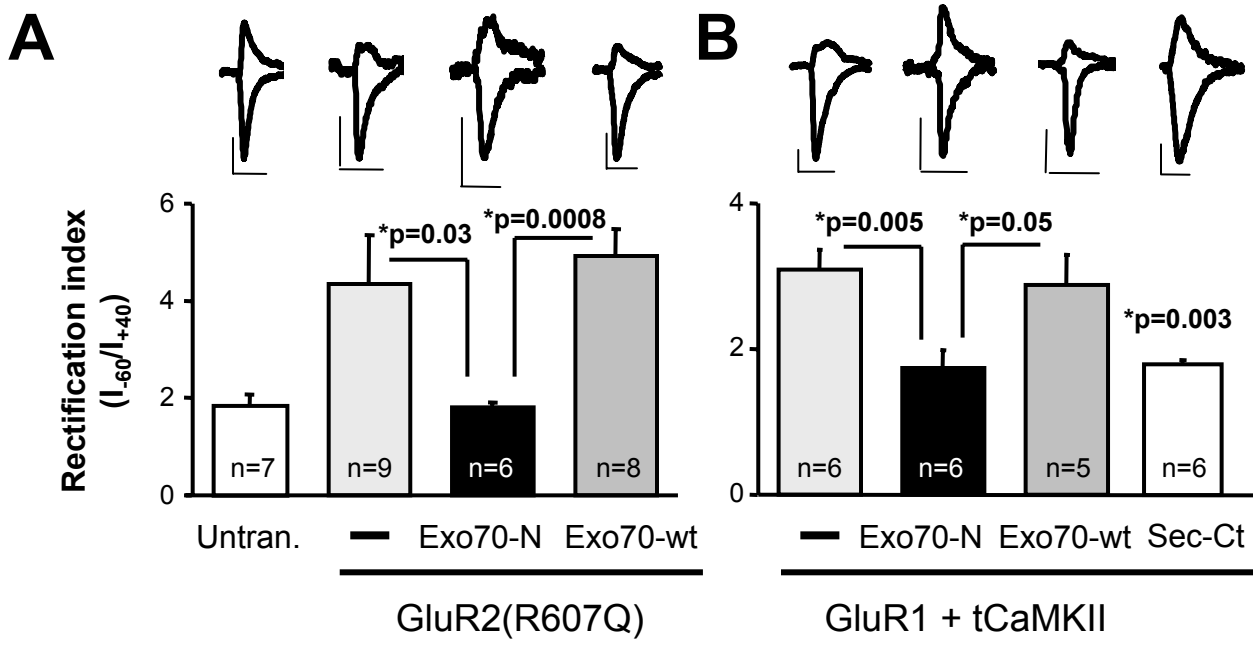

Supplementary Figure 6 (Esteban)